Heliyon 5 (2019) e02828

Contents lists available at ScienceDirect

Heliyon

journal homepage: www.heliyon.com

Heliyon

Research article

Effect of particle sizes on the kinetics of demineralization of snail shell for chitin synthesis using acetic acid

Daniel T. Oyekunle *, James A. Omoleye

Department of Chemical Engineering, College of Engineering, Covenant University, Ota, Nigeria

ARTICLE INFO

Keywords:
Chemical engineering
Materials chemistry
Demineralization
Chitin
Kinetics
Shrinking core model
Acetic acid

ABSTRACT

This study considers the kinetics of snail shells demineralization process using acetic acid. It was washed, sundried then ground into four different particle sizes. The ranges of particle sizes are 6.3–4.75 mm, 4.75–2 mm, 2 - 1 mm, and 600 -300 μm. The shells were first deproteinized with sodium hydroxide solution thereafter they were demineralized using 1.2 M acetic acid solution. Kinetics of demineralization of the snail shells was performed by XRF analysis of the chitin produced at 5, 10, 15, 20, 25, 30, and 35 min. The kinetic results show that mechanism of chitin formation from snail shell occurs through the chemical reaction controlled (CRC) model of the shrinking core model for particle sizes between 6.3 – 4.75 mm, 4.75–2 mm, and 2–1 mm particle sizes while Fluid Film Diffusion (FFD) model was observed for the smaller range of 600–300 μm particle sizes. The surface morphology and the FTIR analysis of the synthesized chitin were typical of those obtained for earlier studies.

1. Introduction

Chitin, poly (β-(1–4)-N-acetyl-D-glucosamine), is a major constituent present in crustaceans shells such as crawfish, krill, crabs, shrimps, and lobsters. It looks similar to (β-(1–4) - anhydroglucopyranose chain present in cellulose with the exception of the acetamide group present at the C-2 position of anhydroglucopyranoside residue (Hosseinnejad and Jafari, 2016). Identical to cellulose, native chitin exists in a crystalline state that is fibrous in nature, i.e. microfibrils. Chitin which is a naturally occurring biopolymer can be seen in various structural forms, depending on its source and biological function. The various forms are differentiated based on the carbohydrate chain arrangement. Antiparallel arrangement of the chains is known as α forms while chains in the parallel arrangement are known as β forms. Two chains occurring in one direction that includes an inverted chain are known as γ-chitin (Ogawa et al., 2010).

Chitin can be found in several organisms skeletal structures, including algae (such as diatoms), Mollusca, Porifera (examples include freshwater and marine sponges), Annelina, Anthozoa (e.g. corals) and Nematoda. It can also be found in several other arthropods; Arachina, Crustacea and Insecta (Brunner et al., 2009). Chitin serves as a covering for arthropods and it's a major constituent in the mushrooms cell wall and also in the structural makeup of other organisms such as nematode, coral and algae. Chitin exists predominantly as cellulose in nature, it has diverse applications in cosmetics, medicine, biotechnology, agriculture and science bio-inspired materials (Oyekunle and Omoleye, 2019a; Park and Kim, 2010).

Several techniques are used by various researchers to characterize the chitin produced and this includes FTIR (Fourier Transform Infra-Red spectroscopy) and SEM (Scanning Electron Microscopy). FTIR spectroscopy is used to characterize the chitin structures. Using FTIR, Kaya et al. (2014) reported α – crystal form in the chitin structure produced from *N. gluca, A. imperator, H piceus, R. linearis,* and *A. bipustulaus*. The chitin extracted by El knidri et al. (2016) shows characteristic α – chitin band at about 1654–1621 cm^{-1} amide split, and 1550 cm^{-1} amide II band.

SEM analysis is usually carried out to determine the chitin surface morphology. Daraghmeh et al. (2011) explained that α – chitin structure usually occurs as several united fine leaves with high porosity. Al Sagheer et al. (2009) reports that α – chitin structure has a dense structure with a lamellar organization, the β – chitin surface appears different and less crystalline when compared with α – chitin. Chitin occurs in different degree of acetylation (DA) that varies from fully acetylated to total deacetylated. The degree of acetylation is a very essential property of chitin due to its effects on its physical properties. For example, an increase in the degree of acetylation decreases the degree of solubility in solvents (Oyekunle, 2019). FTIR spectroscopy can be used to estimate the degree of acetylation.

Due to the chitin compact structure, it is insoluble in most organic solvents and aqueous solutions. Chitin has limited practical applications

* Corresponding author.
E-mail addresses: daniel.oyekunle@covenantuniversity.edu.ng, oyekunledanielt@yahoo.com (D.T. Oyekunle).

https://doi.org/10.1016/j.heliyon.2019.e02828
Received 24 December 2018; Received in revised form 2 November 2019; Accepted 6 November 2019

whereas the artificial variant of chitin – chitosan; is more useful and suitable for potential applications (Dash et al., 2011). Chitosan (the most common chitin derivative) is produced as a result of the partial N-deacetylation of chitin performed by chemical modifications, having more soluble analogs. Chitin and chitosan have continued to attract global interest due to their various advantages such as non-toxicity, biocompatibility, biodegradability, and non-antigenicity (Liu et al., 2012). The potential of the versatile biopolymers in different fields is actively studied. It has been established as a stabilizing, emulsifying, antimicrobial and thickening agent in the food industry (Oyekunle, 2019). Another notable biomedical activity such as immune system enhancement, antimicrobial, hypolipidemic, hemostatic and wound healing activity has been studied (Aranaz et al., 2009). The continuous use of chitin in several industrial applications has necessitated a need to investigate the kinetics of its demineralization process for better optimization, control, and understanding of the process. It's essential to highlight the significance of particle sizes on the demineralization process and thus determine the most effective model for each particle size in the time range considered.

In this study, the shrinking core model (SCM) for fluid particle reactions is considered for the kinetics of the snail shell demineralization process. The SCM involves the visualization of the reaction taking place on the particle. It is seen that the zone of the reaction first takes place on the external surface of the particle, then moves inward into the solid matrix as the reaction progresses. This leaves behind a portion of completely converted external surface area and an inert solid residue referred to as 'ash'. This model has been observed to occur in various situations which include; burning of wood, coal and tightly wrapped papers (Levenspiel, 1999). Since this model seems to occur naturally in a broad range of situations, a kinetic model developed by Levenspiel (1999) was employed in this study. SCM in this study was performed using 1.2M acetic acid as a surrounding fluid while snail shells of different particle sizes were used as the solid particle.

This study aims to establish the mechanism of the demineralization process of chitin. Deproteinization of the raw shells was first carried out to remove proteins present in the shells at a high temperature. The demineralization of the deproteinized shells was carried out at room temperature at a constant stirring speed. The concentration of Ca^{2+} that remains after the reaction were determined and hence the conversion. The resulting conversion versus time data obtained was processed to investigate the reaction controlling mechanism among the fluid film diffusion (FFD), ash layer diffusion (ALD) and the chemical reaction (CRC). The degree of Acetylation of the chitin produced was reported. FTIR and SEM characterization of the chitin produced was discussed and compared with previous studies. This study is the first to report the kinetics of the demineralization of snail shells and to investigate the reaction model for different particle sizes.

2. Materials and methods

2.1. Raw materials

The raw materials used for this study were snail shells (*Archachatina marginata*) purchased in Ipata market, Ilorin, Kwara state, Nigeria. The shells were washed thoroughly with water to remove tissue and dirt, furthermore, the washed shells were sundried for about 2 – weeks, then ground using an industrial grinder. Thereafter, the particle sizes were separated into 6.30–4.75 mm, 4.75–2.00 mm, 2.00–1.00 mm, and 600–300 μm range of particle sizes using mechanical sieve shaker for 5 min. The sieved shells were kept in an air tight container prior to laboratory analysis.

2.2. Demineralization using various particle size

Deproteinization of the raw snail shells was carried out using 2 ml of 1M NaOH solution with 1 g of snail shells for 2 h on a temperature-controlled magnetic stirrer at 80 °C to remove the protein layer that serves as a covering for the mineral matrix. The deproteinization process removes the inorganic portion of the solid material in the shells thereby enhancing the demineralization process. The removal of the inorganic solid portion of the shell results in low yield (Oyekunle, 2019). The product was dried in an oven at 70 °C until a constant weight was achieved. XRF (x-ray fluorescence) analysis performed on the deproteinized shells is illustrated in Fig. 1. 40 g of deproteinized shells were demineralized using 3 ml of 1.2 M acetic acid solution with 1 g of snail shells. This was stirred for 5, 10, 15, 20, 25, 30, and 35 min using a magnetic stirrer with constant revolution per minute at room temperature. At the end of each reaction time, the product was oven-dried at 70 °C and XRF analysis was used to determine the concentration of Ca^{2+} that has reacted with the acetic acid solution.

Fig. 1 shows that CaO content was greater than all other oxide analyzed by the XRF analysis. Since the demineralization process reduces the amount of mineral content (e.g. CaO) present in the shells, XRF analysis was used to determine the CaO content present after each reaction time considered. Hence, this was used to determine the concentration and conversion of Ca^{2+}.

2.3. Kinetic modelling

Kinetic modeling was carried out based on the concentration of Ca^{2+} ion present in the demineralized shell as time increases. A gradual depletion was observed in the concentration of Ca^{2+} present, Ca^{2+} concentration was used to analyze the kinetic modeling of the demineralization reaction. The mechanism of demineralization is investigated through the shrinking core model. The modeling equations when FFD, ALD or CRC controls the rate respectively are shown in Eqs. (1), (2), and (3) as reported by Levenspiel (1999).

$$\frac{t}{\tau} = X_A \tag{1}$$

$$\frac{t}{\tau} = 1 - 3(1 - X_A)^{2/3} + 2(1 - X_A) \tag{2}$$

$$\frac{t}{\tau} = 1 - (1 - X_A)^{1/3} \tag{3}$$

where t is the reaction time, τ is the time required for complete reaction and conversion of Ca^{2+} ion is represented by X_A.

2.4. Degree of acetylation

Infra-red spectroscopy was used to calculate the degree of acetylation of the solid chitin produced. The equation used in this study was based on the absorbance ratios at 1655 cm^{-1} and 3450 cm^{-1} as stated in Eq. (4) (Oyekunle, 2019).

$$DA\ (\%) = \frac{A_{1655}}{A_{3450}} \times 115 \tag{4}$$

3. Results and discussion

3.1. Results on kinetics of demineralization

The concentration of calcium with demineralization time for the various particle sizes of the deproteinized shell is shown in Fig. 2. As illustrated in the figure, it can be seen that for all particle sizes the concentration of Ca^{2+} reduces as reaction time progresses. For lower particle sizes of 600–300 μm the concentration of Ca^{2+} decreases rapidly for the first 5 min, then the concentration reduces gradually as the reaction time progresses. It was observed that for the biggest particle size (6.3–4.75 mm) the concentration of Ca^{2+}gradually reduces at a much lower rate compared to other particle sizes. Therefore, from the plot, it

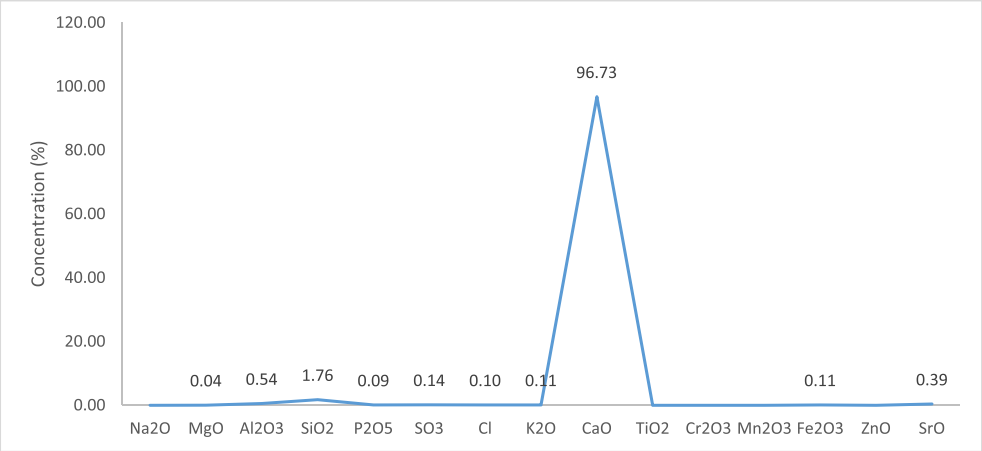

Fig. 1. XRF analysis of the deproteinized snail shells.

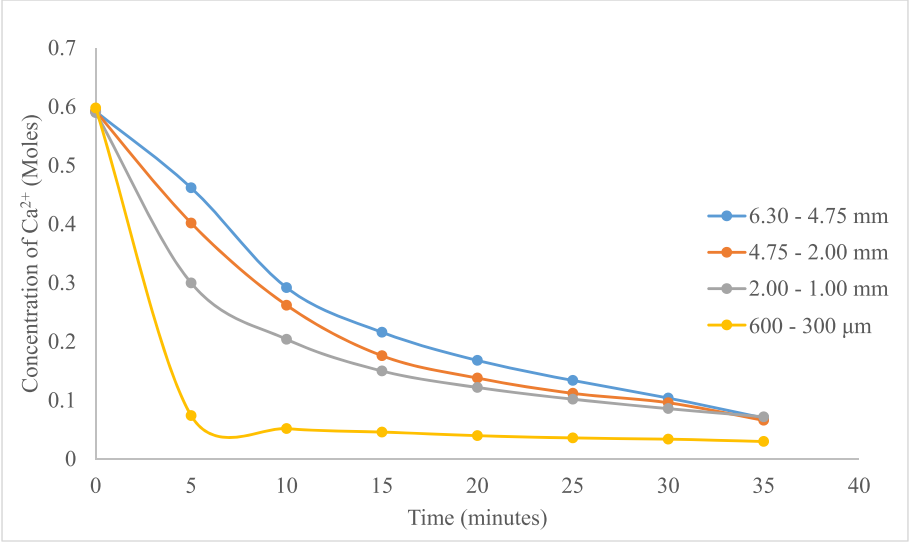

Fig. 2. Effect of 1.2M acetic acid treatment on Ca^{2+} concentration on snail shell demineralization.

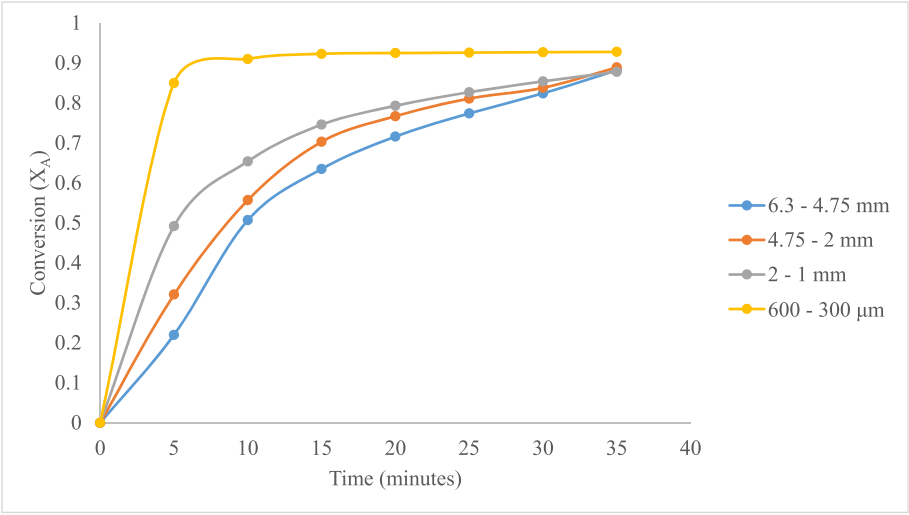

Fig. 3. Effect of 1.2M acetic acid treatment on Ca^{2+} conversion (X_A) in snail shell demineralization.

can be deduced that smaller particle sizes favors rapid reaction while larger particle sizes result in the low conversion of reactants. Fig. 3 shows that for smaller particle sizes of 600–300 μm, there was a rapid conversion of snail shells while larger particle sizes show that the rate of conversion of reactants (snail shells) is lower as the particle sizes gets bigger. But as the reaction progresses they all tend to approach the conversion of 1 (that is a point where all of the reactants would have been converted).

Using the modeling Eqs. (1), (2), and (3) linear graphs for each particle size are plotted as shown in Figs 4, 5, 6 and 7. From the figures shown, the coefficient of determination (R^2) value of each particle size was determined using the shrinking core model. For 6.3–4.75 mm range of particle size (Fig. 4) R^2 values of FFD, CRC and ALD were reported to be 0.8784, 0.9684, and 0.9963 with Standard Error (SE) values of 0.0859, 0.0550, and 0.0649 respectively. Although, the R^2 value for all the models considered were above 0.8, this demonstrate that all models were good in predicting the mechanism of the reaction process taking place in the snail shells but as a result of the lowest standard error values of 0.0550 reported by the CRC, this clearly implies that CRC model gives the best rate of control in the reaction process over the other types of models (i.e. FFD and ALD) considered. Also for 4.75–2 mm range of particle size (Fig. 5), a similar occurrence was observed as R^2 values of FFD, CRC and ALD were reported to be 0.8538, 0.9468, and 0.9795 which demonstrate good predictability with all the R^2 values well above 0.8, but the SE values of 0.0748, 0.0515, and 0.0640 were reported for FFD, CRC and ALD respectively. This implies that CRC best controls the reaction process due to its high R^2 value and having the lowest SE value of 0.0515. Moreover for the 2–1 mm range of particle sizes (Fig. 6) R^2 values of FFD, CRC and ALD were reported to be 0.8657, 0.9433, and 0.9665, which also demonstrates a good predictive efficiency of all the models considered. The SE values of FFD, CRC and ALD are 0.0514, 0.0401, and 0.0535 respectively, CRC has the lowest SE value of 0.0401. This affirms that CRC gives the best prediction among all the models considered for this particle size. In contrast to all the previous particle sizes considered, for 600–300 μm range of particle size (Fig. 7) R^2 values of FFD, CRC and ALD were reported to be 0.9313, 0.9576, and 0.9563, this shows that the predictive capacity of all the models was good. But SE values of 0.0113, 0.0167, and 0.0249 were reported for FFD, CRC and ALD respectively. Therefore as a result of the lowest SE values reported for the FFD model, it can be deduced that for this particle size FFD controls due to its high R^2 value and low SE value. Furthermore, it can be seen that for all the model considered, R^2 values were above 0.8. It was sufficient to state that the model with the lowest SE values controls.

3.2. SEM analysis of chitin produced

The chitin produced was analyzed by FTIR and SEM analysis. The surface morphology of the chitins isolated from snail shells was examined. The chitin has a smooth surface morphology as shown in Fig. 8. Although, the surfaces are of different particle sizes, with some void spaces shown in the background. From the SEM micrographs observed, chitin extracted from snail shells was shown to have a resemblance to those from previous studies by Akpan et al. (2018) and Gbenebor et al. (2017). Microstructural evidence showing different magnifications of the surface morphologies of the chitin produced have been attached as a supplementary file (Fig. S1 – S5).

3.3. FTIR analysis of chitin produced

FTIR analysis of the chitin extracted (Fig. 9) shows the presence of chitin characteristic band at 3618.58, 2850–3000, 1689, 1504 and 1172.76 cm^{-1} which are attributes of O–H, C–H stretching, amide I, II and III respectively. In this study, all these characteristic bands are present and similar to chitin extracted from house cricket and commercial shrimp as reported by Ibitoye et al. (2018). The C–O stretching vibration at 1018 and 1172 cm^{-1} wavenumbers were evaluated for the snail shells chitin in the secondary alcohol. Also, the absorption bands noted at 856.4 cm^{-1} was attributed to monosaccharide rings that were C–H out-of-plane vibration. Nevertheless, the FTIR results suggest a close similarity between the bonding types and chemical composition of shrimp chitins and therefore, can be used as its substitute in other utilities such as chitosan production.

3.4. DA of chitin produced

The biological and chemical properties of chitin largely depend on its DA value. The DA value of chitin extracted from snail shells was calculated to be 126.42 % which was higher than 87.3 % and 99.0 % reported by Kaya et al. (2015) for bumblebee and shrimp respectively. Kaya et al. (2015) noted that chitin with DA values higher than 100%, has some mineral residues available, while for DA values lower than 100% composed of protein residues. The DA values that are above 100% in this study implies that there are some mineral residues that are still available

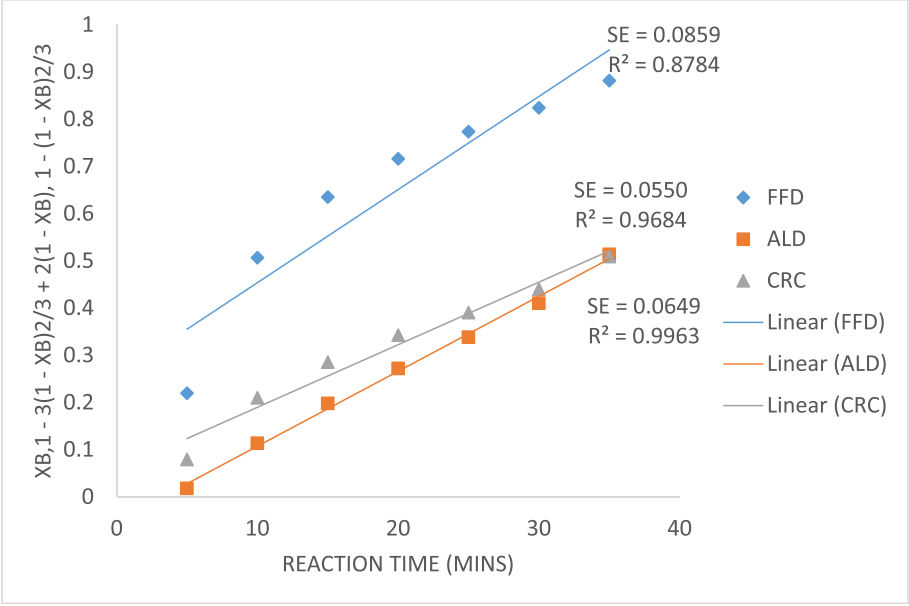

Fig. 4. SCM for 6.30–4.75 mm snail shell particle sizes demineralization using 1.2M acetic acid.

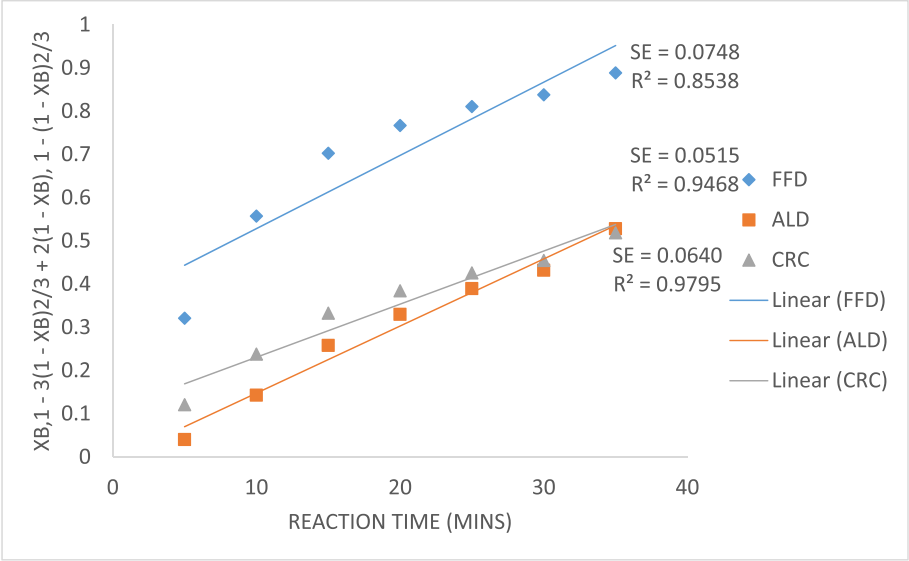

Fig. 5. SCM for 4.75–2.00 mm snail shell particle sizes demineralization using 1.2M acetic acid.

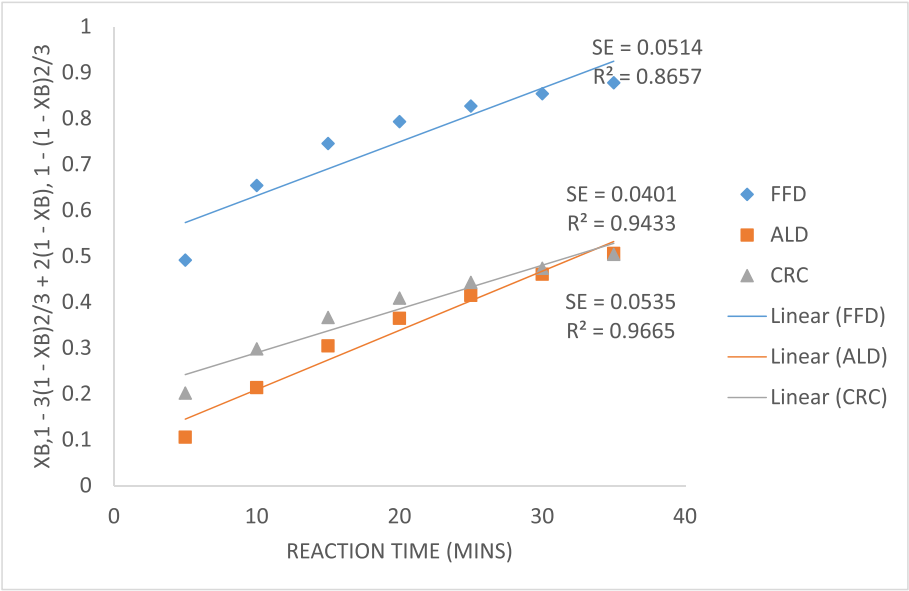

Fig. 6. SCM for 2.00–1.00 mm snail shell particle sizes demineralization using 1.2M acetic acid.

in the chitin. Therefore higher reaction time and higher acid concentration are required to effectively remove all the mineral residue present in the shells in order to attain a DA value of 100 %. Nevertheless, some studies have also reported chitin of higher DA values extracted from various organisms which include; crude chitin (151%), cicada sloughs (102%), rice-filled crab (104%), although it was worthy of note that the use of ^{1}H NMR gave a lower DA of the chitin produced (Sajomsang and Gonil, 2010).

4. Conclusion

It can be concluded that shrinking core models (FFD, ALD, and CRC) models were a good prediction of the demineralization process due to their respective R^2 values which were greater than 0.8. For larger particle sizes (≥1 mm) it can be deduced that ALD R^2 values were greater than those of CRC and FFD, but as a result of the lowest SE values reported for all the CRC models considered in this range of particle sizes. It was noted that although, the necessary condition of having a higher R^2 value of 0.8 was attainted by all the models but the sufficient condition of having the lowest SE values in the following range of particle size 6.3–4.75 mm, 4.75–2 mm and 2–1 mm was attained by CRC therefore, the CRC gives the best prediction to the shrinking core models of snail shells for these particle sizes. As the particle size reduces, the R^2 value of the ALD, CRC and FFD models were still above 0.8. But SE values of FFD was the lowest in comparison to the ALD and CRC models. Therefore, it can be deduced that as the particle sizes reduce FFD is favored over CRC and ALD as the best mechanism of reaction due to the presence of a larger surface area of the solid. SEM and FTIR analysis of the chitin synthesized from snail are typical of what obtains from other chitin sources.

Declarations

Author contribution statement

Daniel T. Oyekunle: Conceived and designed the experiments; Performed the experiments; Analyzed and interpreted the data; Contributed

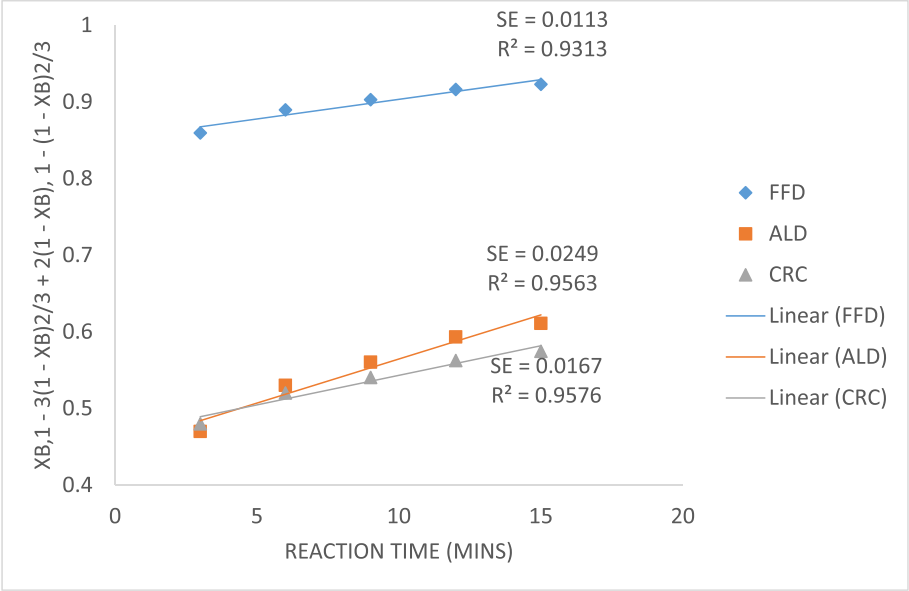

Fig. 7. SCM for 600–300 μm snail shell particle sizes demineralization using 1.2M acetic acid.

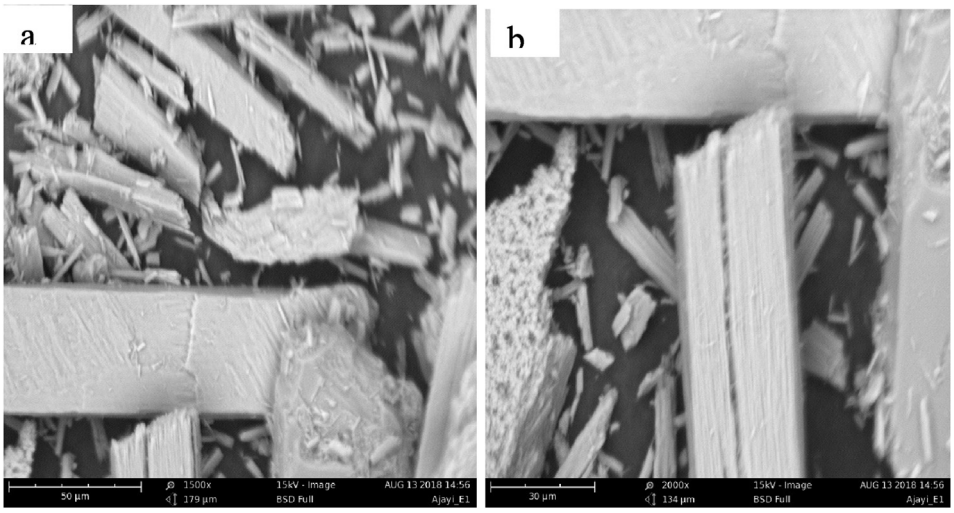

Fig. 8. Surface morphology of the chitin produced at magnifications of 1500x (a) and 2000x (b).

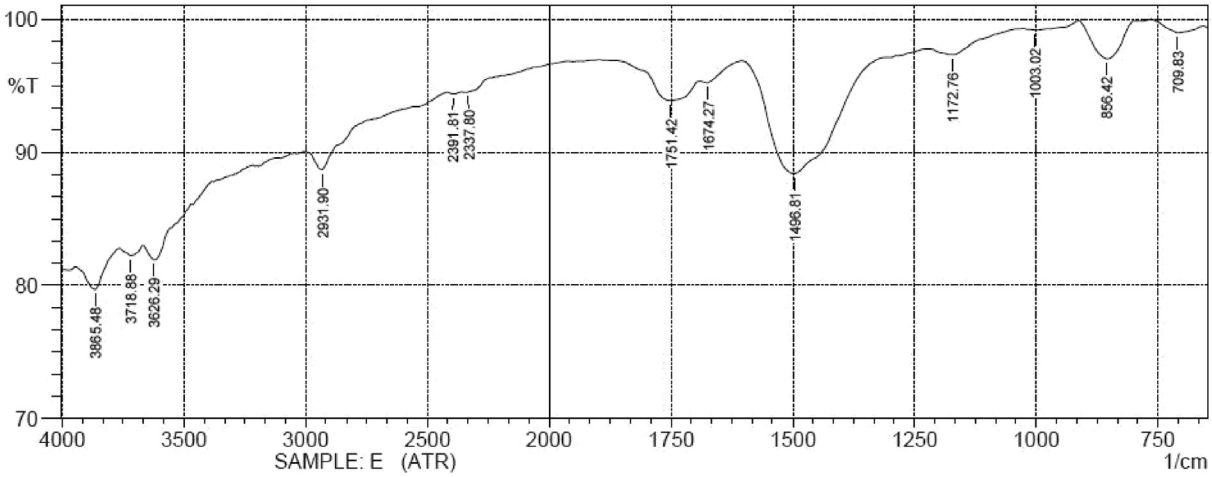

Fig. 9. FTIR spectra of chitin extracted from snail shells.

reagents, materials, analysis tools or data; Wrote the paper.

James A. Omoleye: Conceived and designed the experiments; Analyzed and interpreted the data.

Funding statement

This research did not receive any specific grant from funding agencies in the public, commercial, or not-for-profit sectors.

Competing interest statement

The authors declare no conflict of interest.

Additional information

Supplementary content related to this article has been published online at https://doi.org/10.1016/j.heliyon.2019.e02828.

Acknowledgements

The authors appreciate the effort of Prof. Ayoola O. Ajayi of Ahmadu Bello University for his efforts in ensuring the characterization of the chitin produced in this study. The authors also appreciate Prof. O. O. Ogunleye for proofreading this manuscript. This study is a part of the Corresponding author's master's dissertation.

References

Akpan, E.I., Gbenebor, O.P., Adeosun, S.O., 2018. Synthesis and characterisation of chitin from periwinkle (Tympanotonus fusatus (L.)) and snail (Lissachatina fulica (Bowdich)) shells. Int. J. Biol. Macromol. 106, 1080–1088.

Al Sagheer, F.A.A., Al-Sughayer, M.A., Muslim, S., Elsabee, M.Z., 2009. Extraction and characterization of chitin and chitosan from marine sources in Arabian Gulf. Carbohydr. Polym. 77 (2), 410–419.

Aranaz, I., Mengibar, M., Harris, R., Panos, I., Miralles, B., Acosta, N., Galed, G., Heras, A., 2009. Functional characterization of chitin and chitosan. Curr. Chem. Biol. 3, 203–230.

Brunner, E., Ehrlich, H., Schupp, P., Hedrich, R., Hunold, S., Kammer, M., Machill, S., Paasch, S., Bazhenov, V.V., Kurek, D.V., Arnold, T., Brockmann, S., Ruhnow, M., Born, R., 2009. Chitin-based scaffolds are an integral part of the skeleton of the marine demosponge Ianthella basta. J. Struct. Biol. 168, 539–547.

Daraghmeh, N.H., Chowdhry, B.Z., Leharne, S.A., Al Omari, M.M., Badwan, A.A., 2011. Chapter 2 -chitin In: Profiles of Drug Substances, *Excipients and Related Methodology*, first ed., 36. Elsevier Inc.

Dash, M., Chiellini, F., Ottenbrite, R.M., Chiellini, E., 2011. Chitosan - a versatile semi-synthetic polymer in biomedical applications. Prog. Polym. Sci. 36 (8), 981–1014.

El Knidri, H., El Khalfaouy, R., Laajeb, A., Addaou, A., Lahsini, A., 2016. Eco-friendly extraction and characterization of chitin and chitosan from the shrimp shell waste via microwave irradiation. Process Saf. Environ. Prot. 104, 395–405.

Gbenebor, O.P., Akpan, E.I., Adeosun, S.O., 2017. Thermal, structural and acetylation behavior of snail and periwinkle shells chitin. Prog. Biomater. 6 (3), 97–111.

Hosseinnejad, M., Jafari, M.S., 2016. Evaluation of different factors affecting antimicrobial properties of chitosan. Int. J. Biol. Macromol. 85, 467–475.

Ibitoye, E.B., Lokman, I.H., Hezmee, M.N.M., Goh, Y.M., Zuki, A.B.Z., Jimoh, A.A., 2018. Extraction and physicochemical characterization of chitin and chitosan isolated from house cricket. Biomed. Mater. 13.

Kaya, M., Baran, T., Asan-Ozusaglam, M., Cakmak, Y.S., Tozak, K.O., Mol, A., Mentes, G., Sezen, G., 2015. Extraction and characterization of chitin and chitosan with antimicrobial and antioxidant activities from cosmopolitan Orthoptera species (Insecta). Biotechnol. Bioproc. Eng. 20 (1), 168–179.

Kaya, M., Baran, T., Mentes, A., Asaroglu, M., Sezen, G., Tozak, K.O., 2014. Extraction and characterization of α-chitin and chitosan from six different aquatic invertebrates. Food Biophys. 9 (2), 145–157.

Levenspiel, O., 1999. Chemical Reaction Engineering, third ed. John Wiley and Sons, New York (Chapter 25).

Liu, S., Sun, J., Yu, L., Zhang, C., Bi, J., Zhu, F., Qu, M., Jiang, C., Yang, Q., 2012. Extraction and characterization of chitin from the beetle Holotrichia parallela Motschulsky. Molecules 17, 4604–4611.

Ogawa, Y., Kimura, S., Wada, M., Kuga, S., 2010. Crystal analysis and high-resolutionimaging of microfibrillar -chitin from Phaeocystis. J. Struct. Biol. 171, 111–116.

Oyekunle, D.T., 2019. Extraction and Kinetics of Chitin and Chitosan from Snail Shells. M.Eng. Thesis. Covenant University, Nigeria.

Oyekunle, D.T., Omoleye, J.A., 2019a. New process for synthesizing chitosan from snail shells. J. Phys. Conf. Ser. 1299, 012089.

Park, B.K., Kim, M.M., 2010. Applications of chitin and its derivatives in biological medicine. Int. J. Mol. Sci. 11, 5152–5164.

Sajomsang, W., Gonil, P., 2010. Preparation and characterization of α-chitin from cicada sloughs. Mater. Sci. Eng. C 30 (3), 357–363.